# Approximate 2D inversion of AEM data

**Peter Wolfgram**[1]    **Daniel Sattel**[2]    **Niels B. Christensen**[3]

**Key Words**: airborne electromagnetics, conductivity section, imaging, 2D inversion

## ABSTRACT

Airborne electromagnetic (AEM) data are presently inverted with one-dimensional (1D) models, either as Conductivity Depth Images (CDI) or with full non-linear inversion, to build model sections from concatenated 1D models. If lateral conductivity changes are small, 1D models are justified. However, AEM investigations are often carried out specifically to find localized conductors, and in this case, 1D inversion is inadequate and will often produce artefacts in the model section.

We have developed an approximate two-dimensional (2D) inversion method that deals with laterally inhomogeneous sections. The method is based on the adaptive Born approximation previously applied by one of the authors (NBC) to the interpretation of central-loop ground EM profiles. The technique produces synthetic models with moderate conductivity contrasts and with some improvement over CDI sections. The computing speed is comparable to that of stitched 1D inversions.

An example of processing field data with the approximate 2D inversion method over a massive nickel sulphide deposit shows results that are promising for its routine application on large AEM data sets.

## INTRODUCTION

Presentations of airborne electromagnetic (AEM) data as depth sections and volume visualizations have become important tools in their investigation (Lane et al, 2000; Sattel and Kgotlhang, 2003). Conductivity sections consisting of stitched-together, layered conductivity estimates at each location along the flight line have been constructed from the AEM data using conductivity depth imaging (Liu and Asten, 1993; Wolfgram and Karlik, 1995), approximate one-dimensional (1D) inversion (Christensen, 2002), full non-linear 1D inversion (Christiansen and Christensen, 2003; Sattel, 1998) and, more recently, other 1D techniques (Sattel, 2002).

[1]  *Fugro Airborne Surveys*
    *65 Brockway Road*
    *Floreat WA 6014*
    *Australia*
    *Tel: +61(8)92736400*
    *Fax: +61(8)92736466*
    *Email: pwolfgram@fugroairborne.com.au*

[2]  *Fugro Airborne Surveys*
    *65 Brockway Road*
    *Floreat WA 6014*
    *Australia*
    *Email: dsattel@fugroairborne.com.au*

[3]  *Department of Earth Sciences*
    *Aarhus University*
    *Finlandsgade 8*
    *DK-8200 Aarhus N*
    *Denmark*

The practical application of these techniques has shown their limitations: artefacts are generated around strong lateral gradients in the conductivity distribution, such as around a conductive sulphide body, or along the edges of conductive cover. The airborne system may detect a conductor from a distance before reaching a location directly above the conductor, but the recorded signal is plotted directly underneath the system. A 1D algorithm would then erroneously interpret the causative conductor as a layer underneath the system. Conductivity sections, generated from stitching many of these 1D solutions together, show misleading structures because the assumption of a layered earth is violated near strong lateral conductivity contrasts. Only 2D and 3D algorithms can account for this kind of conductivity distribution in the ground.

Though 3D modelling of EM responses is presently available (Raiche, 1998) and useful in trial-and-error modelling of EM data (Annetts et al., 2003), the computation times involved in forward responses, let alone calculation of derivatives, still deter full non-linear 3D inversion on AEM data sets, although it has been reported for the MT case (Spichak et al., 1999). Approximate 3D inversion methods for synthetic data have been presented by Zhdanov and Fang (1999), for example, and a promising approach has been shown by Tartaras et al. (2001) who were able to keep the computing time for a small grid (14×30×8 cells) down to 25 minutes on an Ultra Sparc 10 station.

We present an approximate 2D inversion method that uses sensitivity functions based on the adaptive Born approximation (Christensen, 1997). The AEM data are first converted to all-time apparent conductivities. The apparent conductivities are then used in two ways: they form the data vector in a linear system used to solve for the 2D conductivities, and they determine the conductivity scaling of the sensitivity functions and thereby the elements of the Jacobian matrix.

We tested the technique successfully on synthetic TEMPEST data (Lane et al., 2000) generated using the program MARCOAIR (Raiche, 1998). The subsequent application of the method to GEOTEM data acquired across the Harmony nickel sulphide deposit showed improvements over conductivity depth imaging. The computing time required was of the same order as that for layered-earth inversions. One week's worth of AEM surveying can be inverted in about one week of computing time on a Pentium-III PC.

## METHOD AND RESULTS

Inverting AEM data to obtain a conductivity distribution at depth requires sensitivity functions (McGillivray et al., 1994; Christensen, 1995). These functions describe the changes of the response of the AEM system as a function of changes in the conductivity of a given volume element at depth. For a given AEM system they are calculated in three dimensions, and then integrated perpendicular to the flight line as well as over the grid cells of a 2D grid, to produce 2D sensitivity functions (Figure 1). The resulting integrated sensitivity functions are tabulated. The inversion program obtains the sensitivities through interpolation in this
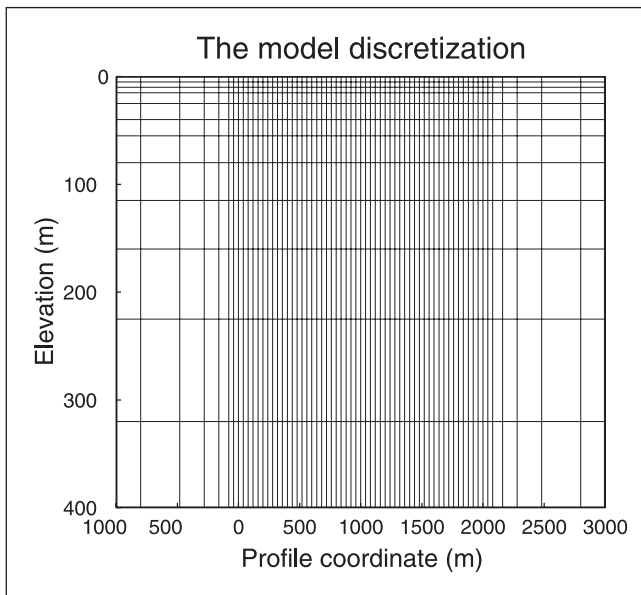
**Fig. 1. The model grid. The outer cells to the left, right, and bottom extend to infinity.**

pre-calculated table, and constructs the coefficient matrix (Jacobian) for a linear system of equations (LSE) which is then solved as a constrained least-squares problem via LU decomposition and back-substitution. The unknown parameters of this LSE are the conductivities of each cell within the 2D grid, and the data vector consists of all AEM data over the portion of the flight line that is covered by the 2D grid.

## Inversion

The 2D model we have implemented has, in the centre portion of the grid, 50 cells horizontally, each 40 m wide, and outer padding cells with increasing widths extending the model to infinity in both directions. Vertically, the model has 12 layers with increasing thickness with depth. This gives a total number of model parameters of 768 and a reasonably fast solution of the inversion problem.

The inversion problem is solved as a constrained least squares problem through

$$\sigma = (\mathbf{A}^{\mathrm{T}} \mathbf{C}_e^{-1} \mathbf{A} + \mathbf{C}_m^{-1})^{-1} \mathbf{A}^{\mathrm{T}} \mathbf{C}_m^{-1} \sigma_a \quad,$$

where $\sigma_a$ is the apparent conductivity data vector, $\mathbf{A}$ is the Jacobian matrix containing the values of the sensitivity function, $\mathbf{C}_e$ is the data error covariance matrix assumed to be diagonal (uncorrelated noise), $\sigma$ is the conductivity of the model elements to be solved for and $\mathbf{C}_m$ is the model covariance matrix correlating the i$^{th}$ and the j$^{th}$ model cell, defined by

$$C_{ij} = C_0 \exp\left[ -\sqrt{\left(\frac{x_i - x_j}{L_x}\right)^2 + \left(\frac{z_i - z_j}{L_z}\right)^2} \right] \quad,$$

where $L_x$ and $L_z$ are the correlation lengths in the x-direction and z-direction, respectively, and $C_0$ is a scaling constant defining the relative weight of the model constraints to the data. We have found that a correlation length of 3000 m in both directions gives the best results in the examples presented.

The 2D grid is moved along the flight line and each time the LSE is solved for the conductivities of the grid cells. To avoid edge effects, there is an overlap between consecutive models and

only the middle 50% of the central portion of the model is used. Finally, all cell conductivities are assembled in a conductivity section display for the entire flight line.

## The adaptive Born approximation

The sensitivity functions of the inversion problem depend on the system configuration, the subsurface model, and the delay time. Throughout the present implementation of the approximate 2D inversion, we use the sensitivity function of the system step response for the homogeneous half-space. The sensitivity functions are shown in Figure 2.

The principle behind the adaptive Born approximation is — for every measuring position and every delay time — to choose the sensitivity function of the half-space with conductivity equal to the all-time apparent conductivity. In this way, the slower diffusion of the electromagnetic field through good conductors, and vice versa for poor conductors, is taken into account (Christensen, 1997).

The sensitivity functions integrated over the model elements are calculated at regularly spaced positions within the central portion of the model. Since the sensitivity function of the step response scales as the time-conductivity ratio, $t/\sigma$, it is calculated over a large range of $\sigma$-values. All values are stored in a binary file to be accessed by the inversion program. These calculations take a few hours on a Pentium III computer, but they are only required once for a given AEM system configuration. A fast, multi-dimensional interpolation in this table is carried out to construct the Jacobian matrix. Interpolation is done along the profile to account for the true position of the data. In this way, all recorded data are used, and spatial interpolation in the data is avoided. At every lateral position, interpolation is carried out in time according to the value of $t/\sigma_a$ at every data point, where $\sigma_a$ is the apparent conductivity of the data. These interpolations are required each time the 2D grid is placed at a new location along the flight line, but take only a fraction of a second.

In the current implementation of the routine, the apparent conductivities are used not only as scaling parameters, but also as data after appropriately scaling the sensitivity functions.

Many definitions of apparent conductivity exist for TEM data (Spies and Eggers, 1986). The one that has proven useful in imaging procedures is the all-time apparent conductivity, derived from the system step response. To find the all-time apparent conductivity from the data would involve a deconvolution with respect to the system response, but since deconvolutions are inherently unstable, we have chosen a different route. For every data set we perform a full non-linear 1D inversion to find a 1D model and in the examples shown below we used the 1D inversion software AIRBEO (Raiche, 1998). The apparent conductivity is then obtained through the generic 1D forward mapping (Christensen, 2002) from 1D conductivity structure to apparent conductivity as a function of time. Note that in this context we are not interested in the similarity between the true conductivity structure and the models obtained from the 1D inversion, only in the fact that the response of the models fits the data and that thereby the forward-calculated apparent conductivity is a good measure of the apparent conductivity.

The approach of finding the apparent conductivity from 1D inversion of the data naturally limits us to cases where data can be fitted with 1D models, i.e., low contrast cases or 'weakly 2D' cases. A highly resistive terrain with localized conductors relatively close to the surface constitutes a 'strongly 2D' case, and 1D models do not fit the data where lateral contrasts are high. In this case, the apparent conductivity determined from 1D inverse modelling must be regarded
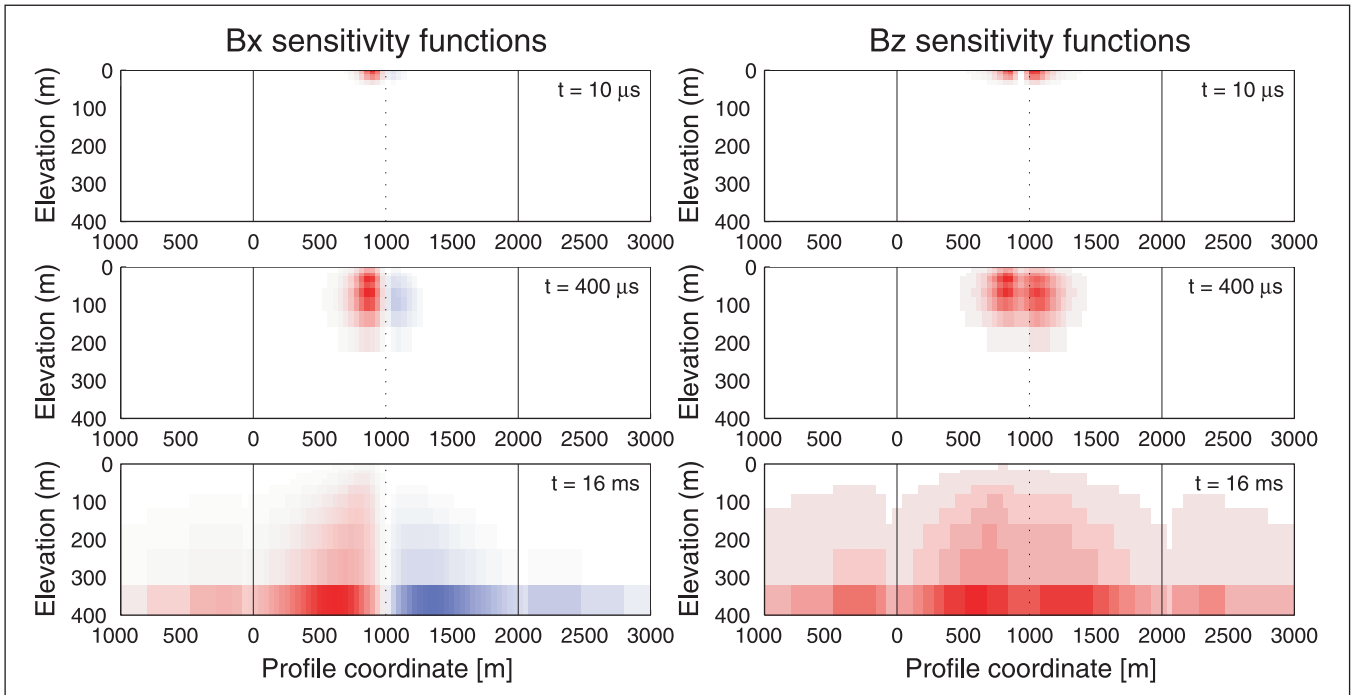
**Fig. 2.** The sensitivity functions at three different delay times of the horizontal and the vertical component for a homogeneous half-space of 10 Ωm integrated over the model elements. Red and blue indicate positive and negative sensitivity, respectively. For the purpose of clarity all plots have been rescaled with the maximum absolute value at every delay time.
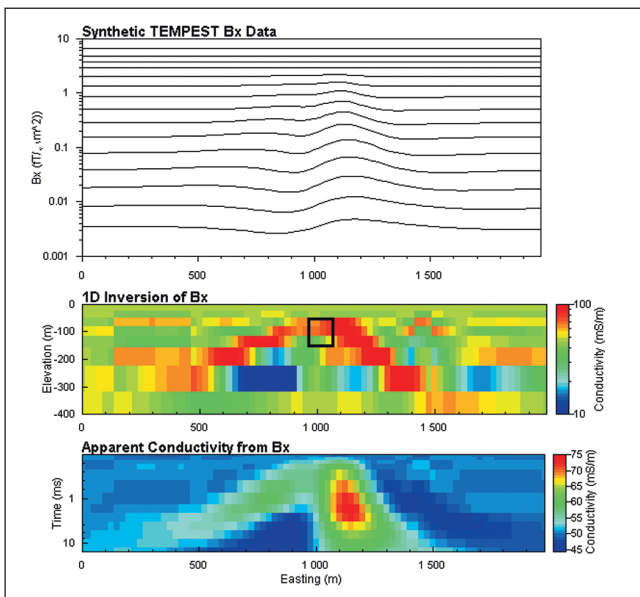


**Fig. 3.** Top: synthetic $B_x$ data for prism model; Middle: 1D inversion result with superimposed outline of the original model; Bottom: calculated apparent conductivity.



**Fig. 4.** Top: synthetic $B_z$ data for prism model; Middle: 1D inversion result with superimposed outline of the original model; Bottom: calculated apparent conductivity.

as an approximation, the best one can do with the current approach. In more conductive terrain, data can most often be fitted with 1D models, and good apparent conductivity estimates can be obtained.

**Test with synthetic data**

Synthetic TEMPEST data generated with the MARCOAIR software (Raiche, 1998) served for an initial validity check of the 2D inversion technique. The model is a 1 km long prism with a 100 m × 100 m cross sectional area and a conductivity of 200 mS/m, situated at a depth (to top) of 50 m below the surface. The prism is situated in a homogeneous half-space with a conductivity 50 mS/m. The synthetic data were inverted using AIRBEO

(Raiche, 1998), and apparent conductivities were calculated from the 1D inversion results. These steps are illustrated in Figure 3 for the horizontal component $B_x$ and in Figure 4 for the vertical component $B_z$.

Neither the 1D sections nor the apparent conductivity images bear any resemblance to the true structure of the original model, but they do show the presence of a buried conductor. Figure 5 shows the 2D inversion result when using the apparent conductivity data of the $B_x$ and $B_z$ components, one at a time and jointly. It is seen that the single use of either component leaves small artefacts in the model sections, that the inversion of $B_x$ alone gives a good result, and that the joint inversion of both components
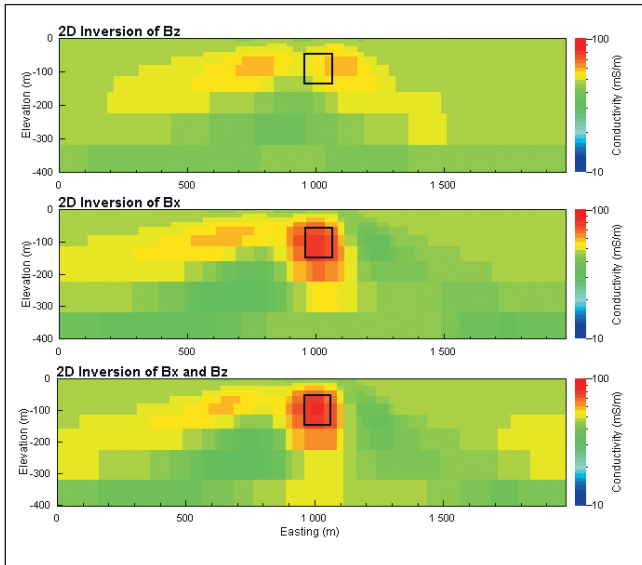
**Fig. 5.** **Top: 2D inversion result from the B$_x$ data only; Middle: 2D inversion result from the B$_z$ data only; Bottom: 2D inversion result from joint inversion of the B$_x$ and B$_z$ data – all with superimposed outline of the original model.**
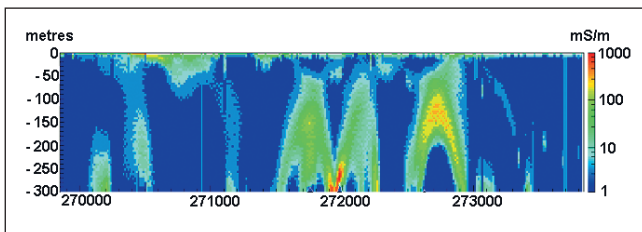


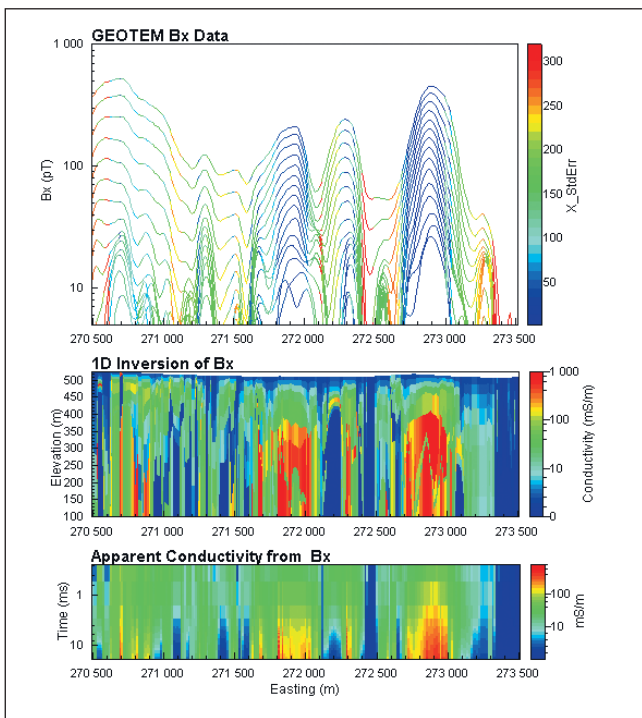**Fig. 6. 1D conductivity-depth image derived from the X-component GEOTEM data.**



**Fig. 7. Result of the 1D inversion of B$_x$. Top: the data profile with the traces colour coded according to the fitting error from the 1D inversion; Middle: the 1D inversion result; Bottom: the calculated apparent conductivity.**

gives the best result. The location of the conductive prism and its approximate shape are recovered, even though its conductivity is underestimated as would be expected using the Born approximation.

## Field example

The 2D inversion was applied to GEOTEM data acquired across the Harmony nickel sulphide deposit in Western Australia (Stolz, 2000). A geological section has been presented in Figure 1 of Wolfgram and Golden (2001). The deposit is located between two conductive shale units dipping towards the west. Wolfgram and Golden (2001) showed that the shape along the profile of both components (B$_x$ and B$_z$) can be explained by a single model of three dipping plate-like conductors. Although successful, the forward modelling with conductive plates was a time-consuming process of multiple model runs and adjustments that required an experienced interpreter. Annetts et al. (2003) obtained a better fit after modelling the same data with 2.5D and full 3D techniques, but they reported between three and 18 hours computing time for each model run on a PC-class computer.

The conductivity-depth image in Figure 6 was generated with program EMFlow (Macnae et al., 1998) and shows the three conductive units. However, neither their locations nor their structural parameters, such as shape and dip of the conductors, are clearly indicated. Instead, some conductive features in the image
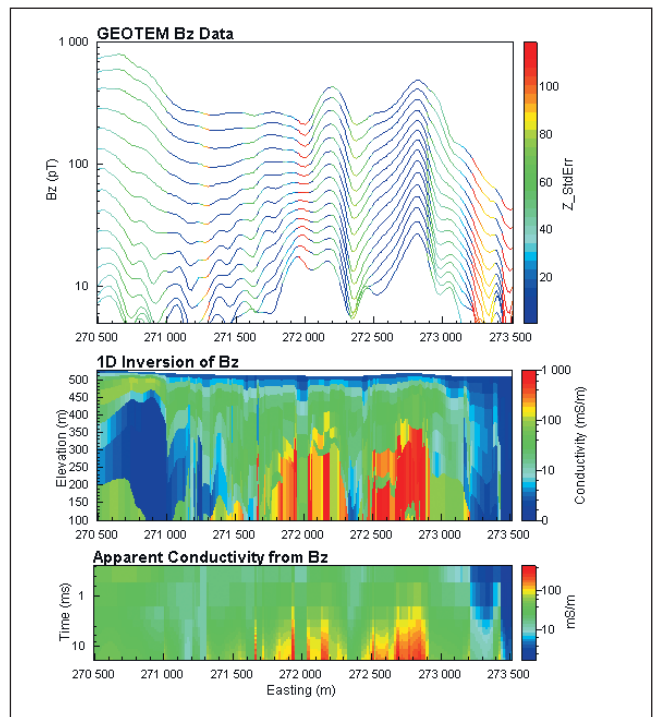


**Fig. 8. Result of the 1D inversion of B$_z$. Top: the data profile with the traces colour coded according to the fitting error from the 1D inversion; Middle: the 1D inversion result; Bottom: the calculated apparent conductivity.**
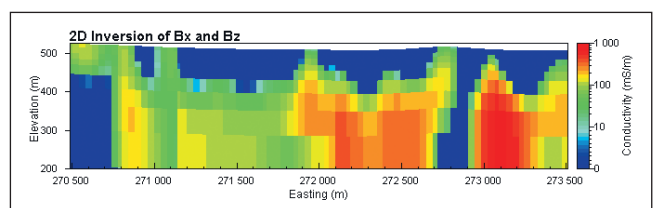


**Fig. 9. Result of the joint 2D inversion of B$_x$ and B$_z$.**

appear to have 'limbs' or 'pant legs' that are reminiscent of diffraction hyperbolas from seismic sections.

The $B_x$ and $B_z$ data are shown in profile form in Figures 7 and 8. We used the fitting error from the 1D inversions for colouring the traces as an indication of where the 1D inversion is invalid. Higher errors are indicated in yellows and reds. The 1D conductivity sections are displayed below the B-field profile data. The Harmony nickel deposit and the neighbouring graphitic shales represent good conductors, with a high conductivity contrast to the host lithologies. The 1D inversion was unsuccessful in reproducing a consistent distribution of conductivity. Even smoothing the data along the profile would only eliminate some of the spurious 1D results, as those data with high fitting errors form groups along the profile that would persist through a smoothing operation.

We attempted a 2D inversion despite the fact that the profile is not 'weakly 2D' to see if a better result could be obtained. The result is shown in Figure 9. Although the structure of three dipping, conductive plates is not resolved in this 2D result, three distinct conductors are visible without the 'pant-leg' artefacts from figure 6. This is an encouraging result considering that our present approach is not strictly valid for this high-contrast 'strongly 2D' case.

The 1D inversions with 9-layer models took just under one hour for each of the two components on a 1GHz Pentium III PC using the AIRBEO program (Raiche, 1998). The 2D inversion of this section required less than 10 minutes to complete on the same computer. The 1D inversion could have been done faster with models with fewer layers, but the multi-layer models have the advantage of being more robust with regard to the choice of initial models for the inversion.

## DISCUSSION

An obvious improvement would be to extend the method to 'strongly 2D' cases to give better conductivity estimates of conductors in high-contrast models, and this development is presently being undertaken. The 'strongly 2D' inversion will be built on an approximate forward mapping as in the 1D case of Christensen (2002). The data vector would then contain the actual measured field data rather than the apparent conductivities. This avoids the 1D inversion that presently limits the technique to cases that can be fitted with 1D models, i.e., to low-contrast cases. However, apparent conductivities would still be required for the conductivity scaling, i.e., to make the Born approximation adaptive. In this regard, a proper mapping from subsurface conductivity to apparent conductivity must be devised. The strategy of an approximate forward mapping has the price that the inversion becomes iterative and not one-pass as in the present approach.

## CONCLUSIONS

We have developed an approximate 2D inversion method based on the adaptive Born approximation that deals with laterally inhomogeneous sections. The method reproduces synthetic models of moderate conductivity contrasts without the artefacts typically seen in CDI sections. The computing speed is comparable to that of stitched 1D inversions.

An example of processing field data over a massive nickel sulphide deposit shows promising results for its routine application on large AEM data sets.

## REFERENCES

Annetts, D., Sugeng, F., and Raiche, A., 2003, Modelling and matching the airborne EM response of Harmony and Maggie Hays: *16th Geophysical Conference and Exhibition, Australian Society of Exploration Geophysicists, Extended Abstracts*.

Christensen N.B., 1995, Imaging of central loop transient electromagnetic soundings: *Journal of Environmental and Engineering Geophysics*, vol. 1, 53–66.

Christensen, N.B., 1997, Electromagnetic subsurface imaging. A case for an adaptive Born approximation: *Surveys in Geophysics*, **18**, 477–510.

Christensen N.B., 2002, A generic 1-D imaging method for transient electromagnetic data: *Geophysics*, **67**, 438–447.

Christiansen A.V., and Christensen N.B., 2003, A quantitative appraisal of airborne and ground-based transient electromagnetic (TEM) measurements in Denmark: *Geophysics*, **68**, 523–534.

Lane, R., Green, A., Golding, C., Owers, M., Pik, P., Plunkett, C., Sattel, D., and Thorn, B., 2000, An example of 3D conductivity mapping using the TEMPEST AEM system: *Exploration Geophysics*, **31**, 162–172.

Liu, G., and Asten, M., 1993, Conductance-depth imaging of airborne TEM data: *Exploration Geophysics*, **24**, 655–662.

McGillivray, P.R., Oldenburg, D.W., Ellis, R.G., and Habashy, T.M., 1994, Calculation of sensitivities for the frequency-domain electromagnetic problem, *Geophysical Journal International*, **116**, 1–4.

Macnae, J., King, A., Stolz, N., Osmakoff, A., and Blaha, A., 1998, Fast AEM processing and inversion: *Exploration Geophysics*, **29**, 163–169.

Raiche, A., 1998, Modelling the time-domain response of AEM systems: *Exploration Geophysics*, **29**, 103–106.

Sattel, D., 1998, Conductivity information in three dimensions: *Exploration Geophysics*, **29**, 157–162.

Sattel D., 2002, Modelling AEM data with Zohdy's method: *72nd Annual International Meeting, Society of Exploration Geophysicists, Expanded Abstracts*.

Sattel, D., and Kgotlhang, L., 2003, Groundwater exploration with AEM in the Boteti area, Botswana: *16th Geophysical Conference and Exhibition, Australian Society of Exploration Geophysicists, Extended Abstracts*.

Spichak, V., Menvielle, M., and Roussignol, M., 1999, Three-dimensional inversion of MT fields using Bayesian statistics: in Oristaglio, M., and Spies, B., (eds.), *Three-dimensional electromagnetics*: Society of Exploration Geophysicists, 406–417.

Spies, B.R., and Eggers, D.E., 1986, The use and misuse of apparent resistivity in electromagnetic methods: *Geophysics*, **51**, 1462–1471. (Errata in *Geophysics*, **53**, 1637)

Stolz, E., 2000, Electromagnetic methods applied to exploration for deep nickel sulphides in the Leinster area, Western Australia: *Exploration Geophysics*, **31**, 222–228.

Tartaras, E., Zhdanov, M., and Balch, S., 2001, Fast 3-D inversion of multi-source array electromagnetic data collected for mineral exploration: *71st Annual International Meeting, Society of Exploration Geophysicists, Expanded Abstracts*, 1439–1442.

Wolfgram, P., and Golden, H., 2001, Airborne EM applied to sulphide nickel - examples and analysis: *Exploration Geophysics*, **32**, 136–140.

Wolfgram, P., and Karlik, G., 1995, Conductivity-depth transform of GEOTEM data: *Exploration Geophysics*, **26**, 179-185, (discussion by Peter Wolfgram: *Exploration Geophysics*, **26**, 549).

Zhdanov, M.S., and Fang, S., 1999, Three-dimensional quasi-linear electromagnetic modelling and inversion: in Oristaglio, M., and Spies, B., (ed.), *Three-dimensional electromagnetics*: Society of Exploration Geophysicists, 233–255.